Short communication: A model to predict flood loss in mountain areas

Sven Fuchs[a],*, Micha Heiser[a], Matthias Schlögl[a], Andreas Zischg[b,c], Maria Papathoma-Köhle[a], Margreth Keiler[b,c]

[a] University of Natural Resources and Life Sciences, Institute of Mountain Risk Engineering, Vienna, Austria
[b] University of Bern, Institute of Geography, Switzerland
[c] University of Bern, Oeschger Centre for Climate Change Research, Mobiliar Lab for Natural Risks, Switzerland

ARTICLE INFO

ABSTRACT

Because effects of climate change and an increase in elements at risk, mountain hazard loss increased throughout Europe. Yet, factors influencing loss, i.e. vulnerability, have gained less attention to date. Vulnerability is defined as the degree of loss resulting from the hazard impact on buildings. Recent studies have focused on evaluating vulnerability to dynamic flooding using proxies from case studies and based on empirical ex-post approaches. However, the transferability to other case studies and, therefore, the ability of such models to actually predict future losses is limited. To overcome this gap, we present a beta model based on loss data from the European Alps, which clearly shows that a single vulnerability function is sufficient to predict losses resulting from different types of torrential hazards and to provide probabilities of destruction under specific scenarios. As a result, the curves are transferable and may significantly increase the predictive power of risk analyses.

1. Introduction

Throughout Europe, increasing losses due to flood hazards have been reported (Kreibich et al., 2014), especially for inundation along large rivers (Barredo, 2007; Di Baldassarre et al., 2018). In contrast, there is a lack of studies on the effects of mountain river flooding (Papathoma-Köhle, 2016; Papathoma-Köhle et al., 2017; Zhang et al., 2018). Increases in overall losses are mainly attributed to the effects of climate change (Mountain Research Initiative EDW Working Group, 2015), which affect the magnitude and frequency of events, and to population dynamics in mountain areas (Fuchs et al., 2015, 2017). However, the vulnerability of communities experiencing the impact of such hazards is less well known (Jakob et al., 2012; Zimmermann and Keiler, 2015), which is also articulated by international frameworks for disaster risk reduction such as the Sendai Framework (UN/ISDR, 2015; Klein et al., 2019), calling for the need for improved understanding of disaster risk in all its dimensions of exposure, vulnerability and hazard characteristics.

Mountain rivers are characterized by dynamic flooding with variable amounts of sediment erosion, deposition and remobilisation (Sturm et al., 2018); typical hazard processes include fluvial sediment transport, debris flows and related phenomena (Slaymaker, 2010; Mazzorana et al., 2014; Karagiorgos et al., 2016; Milanesi et al., 2018). In Europe, such processes repeatedly result in considerable damage to infrastructure and buildings on a local and regional level (Guzzetti et al., 2005; Hilker et al., 2009; Fuchs et al., 2015; Zhang et al., 2018; Zischg et al., 2018; Zou et al., 2018; Schlögl et al., 2019). Several studies used empirical data from past events to assess damage monetarily by using vulnerability functions (Fuchs et al., 2007; Akbas et al., 2009; Quan Luna et al., 2011; Papathoma-Köhle et al., 2012; Sterlacchini et al., 2013), a recent overview is provided in Papathoma-Köhle et al. (2017).

Vulnerability functions are based on the empirical assessment of observed damage and describe underlying process magnitudes and related loss patterns. Consequently, vulnerability ranges from 0 (no damage) to 1 (complete destruction). The use of such vulnerability functions is common in the case of hazards (e.g. river flooding and earthquakes) that affect larger areas and a considerable amount of elements at risk. Nevertheless, despite numerous attempts and models to empirically describe the vulnerability of static flooding along European rivers (Kreibich et al., 2015), such methods and tools are hardly available for assessing the effects of dynamic flooding in mountain watersheds.

Moreover, available data about the empirical assessment of affected buildings located on torrential fans are limited (Papathoma-Köhle et al., 2011, 2017), and were often not found to be transferable to other case studies (Cammerer et al., 2013). On the contrary, there is an emphasis on hazard assessment in specific catchments. The magnitude of these

---

hazard types pose case-specific threats to elements at risk, depending on the geology, catchment and channel morphology, as well as meteorological triggers, and interactions among these factors during an individual event. Recent attempts to derive vulnerability functions using loss data included curve fitting to a series of data that was recorded after major incidents with the aim to predict the probability of occurrence of a certain degree of loss with respect to different flood levels (Papathoma-Köhle et al., 2012; Totschnig and Fuchs, 2013; Carisi et al., 2018). To determine the flood level, deposition height was repeatedly used as a proxy since data on flow velocities were not available (Jakob et al., 2012; Papathoma-Köhle et al., 2015; Chow et al., 2018). The function with the best fit should minimize the squared differences in data, which is consistent with the classical approach of curve fitting; this was repeatedly computed with a Weibull distribution function (Totschnig and Fuchs, 2013; Papathoma-Köhle et al., 2015). As a result, the overall relationship between hazard magnitude and the observed degree of loss can be mirrored. Uncertainties can be expressed by confidence intervals, which depend on the distribution of errors. These uncertainties are of aleatory type and are based on the assumption of symmetrically distributed errors around the mean degree of loss, which is rarely observed in reality. The data spread of Weibull functions results in theoretical loss values below zero and above one, which is inconsistent with the definition of vulnerability. Moreover, the observed loss pattern (Totschnig and Fuchs, 2013; Papathoma-Köhle et al., 2015) is characterized by more data with small values (lower degree of loss) than with high values (larger degree of loss until complete destruction), and the data showed a right-skewed distribution. The larger loss values – and, therefore, the larger degree of loss – tended to be farther away from the mean degree of loss than the smaller values. Hence, a suitable and stochastically valid probability model must be able to model the skewness in the degree of loss. This model requires a parametric assumption and the selection of a suitable probability distribution which enables the statistical treatment of uncertainties. A lack of predictive power of the degree of loss for future events is evident since the current approaches were based on spurious error assumptions (Hastie and Tibshirani, 1990; Fox, 2016).

To overcome this gap, we compiled an integrative dataset that was used to evaluate a model, and which is able to better explain the observed parameter values and the associated skewness. The dataset comprises available data from individual studies conducted in the European Alps (i.e. incidents from Austria and Italy (Fuchs et al., 2007; Fuchs, 2008; Totschnig et al., 2011; Papathoma-Köhle et al., 2012; Totschnig and Fuchs, 2013; Papathoma-Köhle et al., 2015)).

2. Methods

We chose a beta distribution as the underlying model for assessing the vulnerability of buildings. The proposed model assumes that the variable of interest (degree of loss) is continuous, restricted to the interval between zero and one, and is related to the process magnitude through a regression structure (Ferrari and Cribari-Neto, 2004).

The final dataset consists of 214 data points that link observed process magnitudes and the degree of loss for individual buildings damaged during torrent hazards in the European Alps. Additional information about the process subtype (e.g. fluvial sediment transport, hyperconcentrated flow, debris flow), and the type of building was collected. For 60 of the 214 cases investigated, damages occurred due to debris flow hazards, while the remaining 154 damages were caused by fluvial sediment transport and hyperconcentrated flows. The observations were equally distributed over Austria and Italy with 107 cases from each country. Only 10 samples represented commercial buildings and the remaining 204 samples represented residential buildings. The degree of loss was treated as a random variable with values between the interval zero (no loss) and one (complete destruction), hence including the endpoints $[0, 1]$. Therefore, we modelled the influence of the process magnitude ω on the degree of loss with a zero-and-one inflated beta

distribution, which is a mixture of Bernoulli and beta distributions. The resultant density function is given as

$$f(\omega|\mu, \; \sigma, \; \nu, \; \tau) = \begin{cases} \pi_0 & if \; \omega = 0 \\ (1 - \pi_0 - \pi_1)\frac{1}{\mathscr{B}(\alpha,\beta)}\omega^{\alpha-1}(1 - \omega)^{\beta-1} & if \; 0 < \omega < 1 \\ \pi_1 & if \; \omega = 1 \end{cases}$$

(1)

Where $\mu = \alpha/(\alpha + \beta)$, $\sigma = (\alpha + \beta + 1)^{-1/2}$, $\nu = \pi_0/\pi_1$, $\tau = \pi_0/(1 - \pi_0 - \pi_1)$ and $\mathscr{B}(\alpha, \beta)$ is the beta function. The expected value of the distribution is given by $E(\omega) = \frac{\tau+\mu}{1+\nu+\tau}$, see Rigby and Stasinopoulos (2005) and Stasinopoulos and Rigby (2007). To model the dependency of the distribution parameters on the process magnitude, we used a logit link for μ, a log link for ν and τ, while σ was assumed to be constant. The model parameters were estimated by maximizing the log likelihood, using the *gamlss* package (Stasinopoulos and Rigby, 2007) for the statistical software **R** (R Core Team, 2018).

To decide if process magnitude, process type as well as geographical location and building types influence the behavior of the degree of loss, we applied two procedures: (1) a stepwise model selection procedure based on the Generalized Akaike Information Criterion (Akaike, 1974) as the selection criterion, and (2) bootstrapping (i.e. resampling with replacement).

For the first, predictive variables for the regression model were selected by applying bidirectional elimination (i.e. a combination of forward selection and backward elimination) in an iterative process, until the optimal model (i.e. the model with minimal information loss) was found.

For the latter, Eqn. (1) was estimated on 5000 bootstrap samples from the original dataset. For each bootstrap sample the p-value of the explanatory variable was estimated. The number of times variable was significant, hence, the p-value was below 0.05, and was used as a measure of parameter importance (Gilenko and Mironova, 2017).

Uncertainty for the fitted zero-and-one inflated beta distribution was assessed by means of non-parametric bootstrapping, by applying the same analysis steps used for obtaining the final vulnerability function to 5000 new samples generated from the original dataset. From these bootstrap samples, confidence intervals for the regression model were calculated.

3. Results

Bootstrap-based variable selection revealed that there was no need to distinguish between observations regarding geographical location and building type, as the p-values were below 0.05 only in 17% and 13% of all models (Fig. 1, upper left and right). In contrast, the process type was a significant predictor in 58%, and the process magnitude was significant in 100% of all models (Fig. 1, lower left and right). The clear rejection of the geographical location and the building type as potential predictors, the indifferent importance of process type as predictor, and the clear significance of process magnitude supports the hypothesis that a single vulnerability function (depending on the process magnitude) is sufficient to model the degree of loss. This is also mirrored by the large overlap of the boxplots given in the inlet of Fig. 2. These findings are consistent with the stepwise model selection procedure, which resulted in a model featuring process magnitude as the most relevant predictor.

The final model for the mean degree of loss (l_d) as a function of process magnitude is expressed as

$$l_d(\omega) = \begin{cases} 0 & if \; \omega \leq 0 \\ \dfrac{e^{-7.40+2.56\times\omega} + \dfrac{e^{-3.27+1.67\times\omega}}{1+e^{-3.27+1.67\times\omega}}}{1+e^{-9.49\times\omega}+e^{-7.40+2.56\times\omega}} & if \; \omega > 0 \end{cases}$$

(2)

The results are presented in Fig. 2. In the main panel, the process magnitude is shown on the x-axis and the degree of loss on the y-axis. Boxplots were used to indicate the spread in the degree of loss for different process magnitudes observed. The data were summarized into
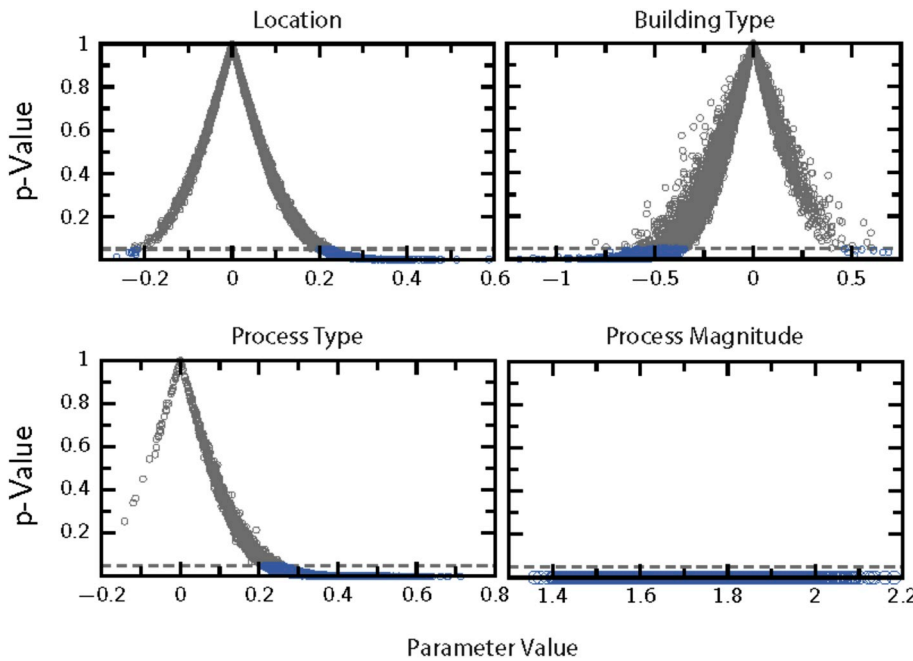
Fig. 1. Upper left and right: The geographical location and building type are insignificant predictors in > 80% of all models, reflected by the large number of points above the dashed line at a p-value of 0.05, shown in grey. Few significant parameter values, shown in blue, provide evidence for an ambiguous influence on the degree of loss, ranging from positive to negative parameter values. Fig. 1, lower left and right: The process type is significant in 58% of all models, with consistently positive parameter values, indicating an increase in the degree of loss for debris flows in comparison to fluvial sediment transport and hyperconcentrated flows if equal process magnitudes are considered. The process magnitude turned out to be a significant predictor in 100% of the models. (For interpretation of the references to colour in this figure legend, the reader is referred to the web version of this article.)

classes of different widths of process magnitudes to ensure a minimum number of five data points for boxplot computation (secondary x-axis). Both the median degree of loss and the spread increase with increasing process magnitude. As a result, three functional relationships can be established: (1) The dashed line represents the probability of an undamaged building (degree of loss = 0) and rapidly decreases with increasing process magnitude, and (2) the dotted line represents the probability of a completely damaged building. This probability remains below 0.1 until a process magnitude of around 2 m and increases significantly thereafter. This is clearly more advantageous when compared to an empirical assessment of vulnerability based on curve fitting. Finally, the black line (3) shows the evolution of the degree of loss for

buildings that are neither fully intact nor totally damaged. The mean degree of loss as a result of the respective process magnitudes is obtained by combining these three components into one mixture model (Eqn. (2)).

In Fig. 3, the expected value of the modelled distribution (c.f. Eqn. (2)) is shown for the entire data range, including no loss and complete destruction. This model includes the process magnitude as the explaining variable and specifically supports the computation of mean losses for buildings affected by torrent events by accounting for data skewness. Consequently, the model shows that once a building is only marginally affected by dynamic flooding, a small degree of loss occurs. Therefore, the model is an extension of an empirical approach that
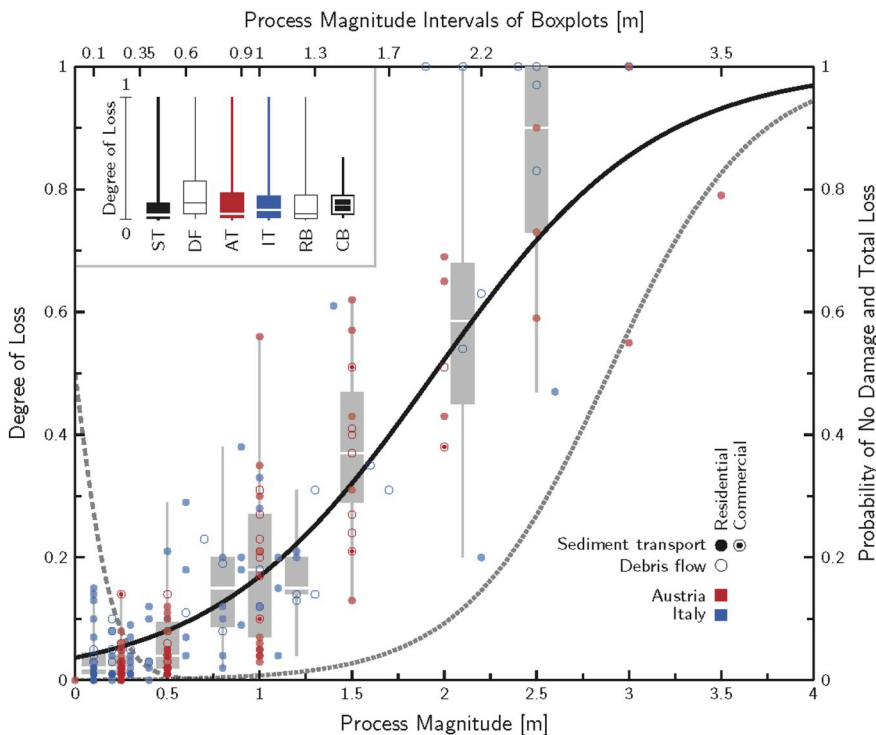

Fig. 2. Three functional relationships based on the zero-and-one inflated beta distribution explain the physical vulnerability of buildings exposed to torrential hazards in the European Alps. The black line shows the mean damage of the underlying beta distribution as a result of different process magnitudes. Additionally, the probability of an undamaged building is shown by the dashed line, and the probability for a building being completely damaged is shown by the dotted line. The underlying equation (1) is presented in the method section. Moreover, the variability of the degree of loss is given for different process types and building categories in the inlet; ST = fluvial sediment transport, DF = debris flow, AT = Austria, IT = Italy, RB = residential building, CB = commercial building. The process magnitude is expressed in terms of deposition heights (i.e. sediment heights deposited around the affected building).
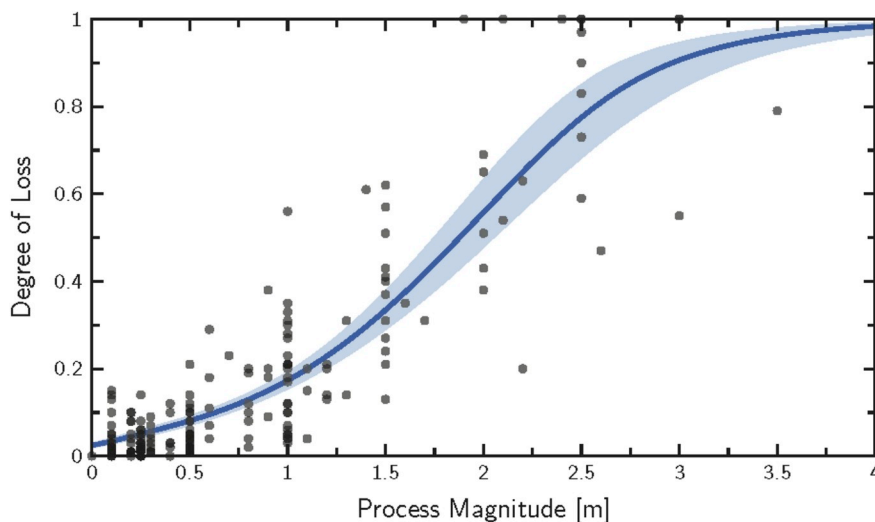
Fig. 3. Mean vulnerability of buildings affected by dynamic flooding from torrential hazards, based on equation (2) (bold blue line), Blue shaded area indicates the 95% confidence interval based on a zero-and-one inflated beta regression model fitted to 5000 bootstrap samples obtained from the original dataset. (For interpretation of the references to colour in this figure legend, the reader is referred to the Web version of this article.)

relies on a normal distribution of the degree of loss, and allows for an ex-ante assessment of damage once potential process magnitudes and the values of elements at risk are known, e.g. from modelling exercises. Uncertainty of the fitted zero-and-one inflated beta distribution is assessed by means of non-parametric bootstrapping (i.e. resampling with replacement). By applying the same analysis steps used for obtaining the final vulnerability function to 5000 new samples generated from the original data set, bootstrap confidence intervals can be calculated for the regression model.

Apart from the uncertainty assessment based on bootstrapping, model quality is assessed by comparing modelled versus observed values of degree-of-loss (Fig. 4). As readily seen, no significant bias towards over- or underestimation is observed, as the 95% confidence area of the regression (blue shaded area) includes the 1:1 line (grey dashed line). Hence, neither the intercept is significantly different from 0, nor the slope is significantly different from 1, even if considerable variability remains. This is also reflected in corresponding error statistics concerning mean squared deviation and its components (Kobayashi and Salam, 2000; Gauch et al., 2003). Based on 5-fold cross validation, translation (squared bias = 0.0004), rotation (non-unity slope = 0.0011) and scatter (lack of correlation = 0.0106) between model-based predictions and observations result in a RMSE of 0.1095 and a MAE of 0.0737.

4. Discussion and conclusion

We extended available studies on the physical vulnerability of buildings to dynamic flooding due to torrential processes to achieve a robust prediction of losses. An improved vulnerability function is presented, derived from a considerable volume of empirical data in comparison to available studies; it is capable of predicting torrential hazard losses in different countries and for various building types. While earlier attempts were only focused on representing the mean degree of loss for different process magnitudes observed, our approach allows risk managers to model future losses as a function of possible impacts due to the deposition of material (and water) on the building envelope. Additionally, the model considers the probability of no loss and the complete destruction of affected buildings. Due to its predictive power, the approach may be applied to operational risk management and also in areas were empirical data is currently not available. The latter is of particular importance; due to climate and socioeconomic changes, the impacts of mountain floods are expected in areas with limited to no records of such previous events. Knowledge of probabilities supports decision making and the prioritization of resources for the construction and implementation of protection measures. Thus, the inclusion of such predictions into future planning processes will further enhance the reliability of vulnerability assessments. Future research may focus on (1) increasing the overall amount of data that can improve and update vulnerability functions, and (2) considering other explaining variables besides deposition height (e.g. flow velocity).

Author contributions

S.F. initiated this work and contributed with loss data from the Austrian Alps, M.H. and M.S. performed the statistical analysis and programmed the loss model with support from S.F. and A.Z.; and M.K., M.P.-K., and A.Z. contributed with loss data from the Italian Alps. All authors were jointly involved with writing the manuscript. Raw data may be obtained from the corresponding author (S.F.). The model is
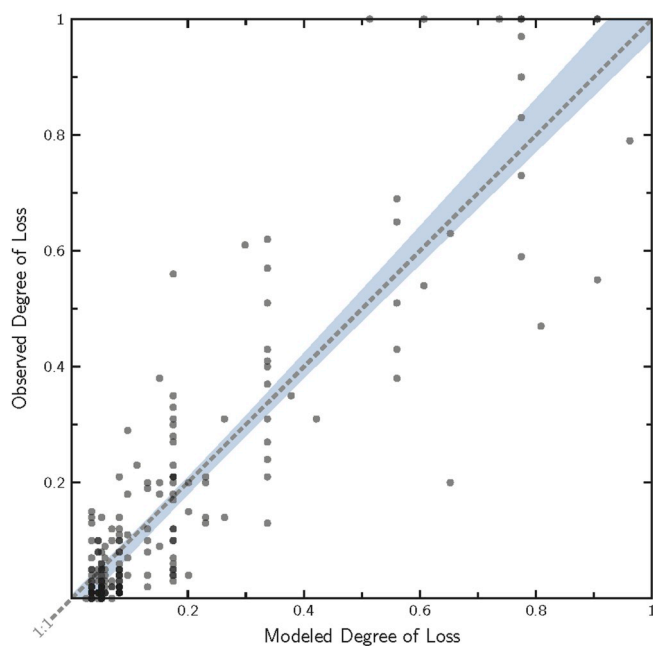

Fig. 4. Evaluation of model results showing predicted versus observed degree-of-loss values. The grey dashed line indicates x = y, i.e. a 1:1 fit. The blue shaded area shows the 95% confidence interval of the linear regression of observed on predicted values, indicating no systematic deviation from the model as the intercept is not significantly different from 0, as well as the slope is not significantly different from 1. (For interpretation of the references to colour in this figure legend, the reader is referred to the Web version of this article.)

available as electronic supplement.

Competing interests

The authors declare no competing interests.

Acknowledgements

Appendix A. Supplementary data

Supplementary data to this article can be found online at https://doi.org/10.1016/j.envsoft.2019.03.026.

References

Akaike, H., 1974. A new look at the statistical model identification. IEEE Trans. Autom. Control 19 (6), 716–723. https://doi.org/10.1109/TAC.1974.1100705.

Akbas, S., Blahut, J., Sterlacchini, S., 2009. Critical assessment of existing physical vulnerability estimation approaches for debris flows. In: Malet, J., Remaître, A., Bogaard, T. (Eds.), Landslide Processes: from Geomorphological Mapping to Dynamic Modelling. CERG Editions, Strasbourgh, pp. 229–233.

Barredo, J., 2007. Major flood disasters in Europe: 1950-2005. Nat. Hazards 42 (1), 125–148. https://doi.org/10.1007/s11069-006-9065-2.

Cammerer, H., Thieken, A., Lammel, J., 2013. Adaptability and transferability of flood loss functions in residential areas. Nat. Hazards Earth Syst. Sci. 13 (11), 3063–3081. https://doi.org/10.5194/nhess-13-3063-2013.

Carisi, F., Schröter, K., Domeneghetti, A., Kreibich, H., Castellarin, A., 2018. Development and assessment of uni- and multivariable flood loss models for Emilia-Romagna (Italy). Nat. Hazards Earth Syst. Sci. 18 (7), 2057–2079. https://doi.org/10.5194/nhess-18-2057-2018.

Chow, C., Ramirez, J.A., Keiler, M., 2018. Application of sensitivity analysis for process model calibration of natural hazards. Geosciences 8 (6), 218. 28 pages. https://doi.org/10.3390/geosciences8060218.

Di Baldassarre, G., Nohrstedt, D., Mård, J., Burchardt, S., Albin, C., Bondesson, S., Breinl, K., Deegan, F.M., Fuentes, D., Lopez, M.G., Granberg, M., Nyberg, L., Nyman, M.R., Rhodes, E., Troll, V., Young, S., Walch, C., Parker, C.F., 2018. An integrative research framework to unravel the interplay of natural hazards and vulnerabilities. Earth's Future 6 (3), 305–310. https://doi.org/10.1002/2017EF000764.

Ferrari, S., Cribari-Neto, F., 2004. Beta regression for modelling rates and proportions. J. Appl. Stat. 31 (7), 799–815. https://doi.org/10.1080/0266476042000214501.

Fox, J., 2016. Applied Regression Analysis and Generalized Linear Models. Sage Publications, London.

Fuchs, S., 2008. Vulnerability to torrent processes. In: Brebbia, C., Beriatos, E. (Eds.), Risk Analysis VI. WIT Transactions on Information and Communication Technologies 39. WIT, Southampton, pp. 289–298. https://doi.org/10.2495/RISK080291.

Fuchs, S., Heiss, K., Hübl, J., 2007. Towards an empirical vulnerability function for use in debris flow risk assessment. Nat. Hazards Earth Syst. Sci. 7 (5), 495–506. https://doi.org/10.5194/nhess-7-495-2007.

Fuchs, S., Keiler, M., Zischg, A., 2015. A spatiotemporal multi-hazard exposure assessment based on property data. Nat. Hazards Earth Syst. Sci. 15 (9), 2127–2142. https://doi.org/10.5194/nhess-15-2127-2015.

Fuchs, S., Röthlisberger, V., Thaler, T., Zischg, A., Keiler, M., 2017. Natural hazard management from a coevolutionary perspective: exposure and policy response in the European Alps. Ann. Assoc. Am. Geogr. 107 (2), 382–392. https://doi.org/10.1080/24694452.2016.1235494.

Gauch, H.G., Hwang, J.T.G., Fick, G.W., 2003. Model evaluation by comparison of model-based predictions and measured values. Agron. J. 95, 1442–1446.

Gilenko, E.V., Mironova, E.A., 2017. Modern claim frequency and claim severity models: an application to the Russian motor own damage insurance market. Cogent Economics and Finance 5 (1311097), 12. (online). https://doi.org/10.1080/23322039.2017.1311097.

Guzzetti, F., Salvati, P., Stark, C., 2005. Historical evaluation of flood and landslide risk to the population of Italy. Environ. Manag. 36 (1), 15–36. https://doi.org/10.1007/s00267-003-0257-1.

Hastie, T.J., Tibshirani, R.J., 1990. Generalized Additive Models. Chapman and Hall, London.

Hilker, N., Badoux, A., Hegg, C., 2009. The Swiss flood and landslide damage database 1972-2007. Nat. Hazards Earth Syst. Sci. 9 (3), 913–925. https://doi.org/10.5194/nhess-9-913-2009.

Jakob, M., Stein, D., Ulmi, M., 2012. Vulnerability of buildings to debris flow impact. Nat. Hazards 60 (2), 241–261. https://doi.org/10.1007/s11069-011-0007-2.

Karagiorgos, K., Thaler, T., Heiser, M., Hübl, J., Fuchs, S., 2016. Integrated flash flood vulnerability assessment: insights from East Attica, Greece. J. Hydrol. 541 (Part A), 553–562. https://doi.org/10.1016/j.jhydrol.2016.02.052.

Klein, J.A., Tucker, C.M., Steger, C.E., Nolin, A., Reid, R., Hopping, K.A., Yeh, E.T., Pradhan, M.S., Taber, A., Molden, D., Ghate, R., Choudhury, D., Alcántara-Ayala, I.,

Lavorel, S., Müller, B., Grêt-Regamey, A., Boone, R.B., Bourgeron, P., Castellanos, E., Chen, X., Dong, S., Keiler, M., Seidl, R., Thorn, J., Yager, K., 2019. An integrated community and ecosystem-based approach to disaster risk reduction in mountain systems. Environ. Sci. Policy 94, 143–152. https://doi.org/10.1016/j.envsci.2018.12.034.

Kobayashi, K., Salam, M.U., 2000. Comparing simulated and measured values using mean squared deviation and its components. Agron. J. 92, 345–352.

Kreibich, H., Bubeck, P., Van Vliet, M., De Moel, H., 2015. A review of damage-reducing measures to manage fluvial flood risks in a changing climate. Mitig. Adapt. Strategies Glob. Change 20 (6), 967–989. https://doi.org/10.1007/s11027-014-9629-5.

Kreibich, H., van den Bergh, J.C.J.M., Bouwer, L.M., Bubeck, P., Ciavola, P., Green, C., Hallegatte, S., Logar, I., Meyer, V., Schwarze, R., Thieken, A.H., 2014. Costing natural hazards. Nat. Clim. Change 4, 303–306.

Mazzorana, B., Simoni, S., Scherer, C., Gems, B., Fuchs, S., Keiler, M., 2014. A physical approach on flood risk vulnerability of buildings. Hydrol. Earth Syst. Sci. 18 (9), 3817–3836. https://doi.org/10.5194/hess-18-3817-2014.

Milanesi, L., Pilotti, M., Belleri, A., Marini, A., Fuchs, S., 2018. Vulnerability to flash floods: a simplified structural model for masonry buildings. Water Resour. Res. 54 (10), 7177–7197. https://doi.org/10.1029/2018WR022577.

Mountain Research Initiative EDW Working Group, 2015. Elevation-dependent warming in mountain regions of the world. Nat. Clim. Change 5, 424–430. https://doi.org/10.1038/NCLIMATE2563.

Papathoma-Köhle, M., 2016. Vulnerability curves vs. vulnerability indicators: application of an indicator-based methodology for debris-flow hazards. Nat. Hazards Earth Syst. Sci. 16 (8), 1771–1790. https://doi.org/10.5194/nhess-16-1771-2016.

Papathoma-Köhle, M., Gems, B., Sturm, M., Fuchs, S., 2017. Matrices, curves and indicators: a review of approaches to assess physical vulnerability to debris flows. Earth Sci. Rev. 171, 272–288. https://doi.org/10.1016/j.earscirev.2017.06.007.

Papathoma-Köhle, M., Kappes, M., Keiler, M., Glade, T., 2011. Physical vulnerability assessment for alpine hazards: state of the art and future needs. Nat. Hazards 58 (2), 645–680. https://doi.org/10.1007/s11069-010-9632-4.

Papathoma-Köhle, M., Keiler, M., Totschnig, R., Glade, T., 2012. Improvement of vulnerability curves using data from extreme events: debris flow event in South Tyrol. Nat. Hazards 64 (3), 2083–2105. https://doi.org/10.1007/s11069-012-0105-9.

Papathoma-Köhle, M., Zischg, A., Fuchs, S., Glade, T., Keiler, M., 2015. Loss estimation for landslides in mountain areas - an integrated toolbox for vulnerability assessment and damage documentation. Environ. Model. Softw 63, 156–169. https://doi.org/10.1016/j.envsoft.2014.10.003.

Quan Luna, B., Blahut, J., van Westen, C., Sterlacchini, S., van Asch, T., Akbas, S., 2011. The application of numerical debris flow modelling for the generation of physical vulnerability curves. Nat. Hazards Earth Syst. Sci. 11 (7), 2047–2060. https://doi.org/10.5194/nhess-11-2047-2011.

R Core Team, 2018. R: A Language and Environment for Statistical Computing. R Foundation for Statistical Computing, Vienna, Austria. https://www.R-project.org/.

Rigby, R.A., Stasinopoulos, D.M., 2005. Generalized additive models for location, scale and shape. Appl. Stat. 54 (3), 507–554.

Schlögl, M., Richter, G., Avian, M., Thaler, T., Heiss, G., Lenz, G., Fuchs, S., 2019. On the nexus between landslide susceptibility and transport infrastructure – an agent-based approach. Nat. Hazards Earth Syst. Sci. 19 (1), 201–219. https://doi.org/10.5194/nhess-19-201-2019.

Slaymaker, O., 2010. Mountain hazards. In: Alcántara-Ayala, I., Goudie, A. (Eds.), Geomorphological Hazards and Disaster Prevention. Cambridge University Press, Cambridge, pp. 33–47.

Stasinopoulos, D.M., Rigby, R.A., 2007. Generalized additive models for location, scale and shape (GAMLSS) in R. J. Stat. Softw. 23 (7), 46. (online). https://www.jstatsoft.org/article/view/v023i007. https://doi.org/10.18637/jss.v023.i07.

Sterlacchini, S., Akbas, S.O., Blahut, J., Mavrouli, O.-C., Garcia, C., Quan Luna, B., Corominas, J., 2013. Methods for the characterization of the vulnerability of elements at risk. In: van Asch, T., Corominas, J., Greiving, S., Malet, J.-P., Sterlacchini, S. (Eds.), Mountain Risks: from Prediction to Management and Governance. Springer, Dordrecht, pp. 233–273.

Sturm, M., Gems, B., Keller, F., Mazzorana, B., Fuchs, S., Papathoma-Köhle, M., Aufleger, M., 2018. Understanding the dynamics of impacts at buildings caused by fluviatile sediment transport processes. Geomorphology 321, 45–59. https://doi.org/10.1016/j.geomorph.2018.08.016.

Totschnig, R., Fuchs, S., 2013. Mountain torrents: quantifying vulnerability and assessing uncertainties. Eng. Geol. 155, 31–44. https://doi.org/10.1016/j.enggeo.2012.12.019.

Totschnig, R., Sedlacek, W., Fuchs, S., 2011. A quantitative vulnerability function for fluvial sediment transport. Nat. Hazards 58 (2), 681–703. https://doi.org/10.1007/s11069-010-9623-5.

UN/ISDR, 2015. Sendai Framework for Disaster Risk Reduction 2015-2030. United Nations, Geneva.

Zhang, S., Zhang, L., Li, X., Xu, Q., 2018. Physical vulnerability models for assessing building damage by debris flows. Eng. Geol. 247, 145–158. https://doi.org/10.1016/j.enggeo.2018.10.017.

Zimmermann, M., Keiler, M., 2015. International frameworks for disaster risk reduction: useful guidance for sustainable mountain development? Mt. Res. Dev. 35 (2), 195–202. https://doi.org/10.1659/MRD-JOURNAL-D-15-00006.1.

Zischg, A., Hofer, P., Mosimann, M., Röthlisberger, V., Ramirez, J.A., Keiler, M., Weingartner, R., 2018. Flood risk (d)evolution: disentangling key drivers of flood risk change with a retro-model experiment. Sci. Total Environ. 639, 195–207. https://doi.org/10.1016/j.scitotenv.2018.05.056.

Zou, Q., Cui, P., Zhou, G.G.D., Li, S.S., Tang, J.X., Li, S., 2018. A new approach to assessing vulnerability of mountain highways subject to debris flows in China. Prog. Phys. Geogr. 42 (3), 305–329. https://doi.org/10.1177/0309133318770985.